

Gradient Theory of Damage Coupled to Frictional Contact and Wear, and Its Numerical Treatment

Peter J. Ireman, Anders Klarbring¹ and Niclas Strömberg

Abstract: In this paper finite element approaches for fretting fatigue are proposed on the basis of a non-local model of continuum damage coupled to friction and wear. The model is formulated in the frame-work of a standard material. In a previous paper this was done in the spirit of Maugin, where an extra entropy flux is introduced in the second law in order to include the gradient of the internal variable in a proper manner. In this paper we follow instead the ideas of Frémond and others, where this extra entropy flux is no longer needed, but instead new non-classical balance laws associated to damage, friction and wear, respectively, are derived from the principle of virtual power. The standard material is then defined as usual by state laws based on free energies and complementary laws based on dissipation potentials. In particular, we pick free energies and dissipation potentials that correspond to a non-local continuum damage model coupled to friction and wear. In addition, the boundary conditions at the contact interface creates a coupling between damage and wear. This is a key feature of our model, which makes it very useful in studies of fretting fatigue. By starting from a variational formulation of the governing equations, two different finite element algorithms are implemented. Both algorithms are based on a Newton method for semi-smooth equations. In the first algorithm the Newton method is applied to the entire system of equations, while in the second algorithm the system of equations is split into two different parts such that an elastic wear problem is solved for fixed damage followed by the solution of the damage evolution problem for the updated displacements and contact forces in an iterative process. The latter algorithm can be viewed as a Gauss-Seidel scheme. The numerical performance of the algorithms is investigated for three two-dimensional examples of increasing complexity. Based on the numerical solutions, the behavior of the model is also discussed. For instance, it is shown numerically how the initiation of damage depends on the contact geometry, the coefficient of friction and the evolution of wear.

¹ Division of Mechanics, Linköping University, SE-581 83 Linköping, Sweden, e-mail: anders.klarbring@liu.se

Keywords: gradient damage, wear, finite element algorithms

1 Introduction

Fretting occurs when two bodies are subjected to small relative oscillatory displacements. It is well-known that under partial slip fretting conditions, the fatigue performance of the bodies is drastically reduced. This reduction is believed to be due to the steep stress gradients appearing in the vicinity of a frictional contact, but seems also to depend strongly on the amount of accumulated slip (Hills and Nowell, 1994). In the present paper this phenomenon is studied using a continuum model, which is non-classical both with respect to the bulk material and the contact interface.

The model of the bulk material is based on a continuum damage model including the gradient of the damage variable, similar to the models of brittle damage suggested and studied by Frémond and Nedjar (1996) and Nedjar (2001). When the gradient of the damage variable is included, the evolution of damage is governed by a boundary-value problem instead of a local evolution law. Besides that the well-known problem with mesh dependent solutions is removed, boundary conditions to the evolution problem can be used to include couplings between bulk damage and processes at the boundary. In the model considered here, such a coupling is suggested between bulk damage and wear. This coupling represents the fact that the fretting conditions reduces the fatigue performance depending on the accumulated relative slip. Furthermore, the behaviour of the contact interface is governed by Signorini's contact conditions, Coulomb's law of friction and Archard's law of wear.

The model of the contact interface including the above mentioned coupling was first derived in Ireman et al. (2003). It relies on the notion of a material interface, introduced by Frémond (1987, 1988) for adhesion coupled to unilateral contact: a view adopted also in studies of unilateral frictional contact in Klarbring (1990), frictional heat generation in Johansson and Klarbring (1993), unilateral frictional contact coupled to wear in Strömberg et al. (1996) and adhesion coupled to unilateral frictional contact in Raous et al. (1999) and Talon and Curnier (2003).

In Ireman et al. (2003) we based the derivation of the model on the introduction of an extra entropy flux as suggested by Maugin (1990). A conceptually different approach, leading to essentially the same equations, was used in Frémond and Nedjar (1996). Here the damage variable is viewed as a microscopic velocity field, which must be accomplished by a balance of associated forces, much in the same spirit as advocated by Gurtin (2000) in his treatment of configurational forces. In the present paper we use such an approach for deriving the model in Ireman et al. (2003). It

involves including all kinematic variables (displacement, damage, slip and wear) in the virtual work equation, leading to non-classical balance equations for associated forces, instead of treating damage, slip and wear as internal processes. This seems to be the more unified treatment, which is more easily extended to, e.g., inclusion of wear debris transportation.

In additions to including a new derivation of the model in Ireman et al. (2003), the present paper also concerns its numerical treatment. We propose numerical methods that are based on a Newton method for non-smooth equations suggested by Pang (1990). This method has been successfully applied to elastic frictional contact problems (Christensen et al., 1998; Christensen and Pang, 1998), elastic wear problems (Strömberg, 1997, 1999), thermo-elastic wear problems (Strömberg, 1998; Ireman et al., 2002), rigid body impact problems (Johansson and Klarbring, 2000), elasto-plastic problems with and without contact (Christensen, 2002a,b), gradient damage problems without contact (Ireman, 2005), impact problems with wear (Strömberg, 2003) and finally large rotation contact/impact problems (Strömberg, 2005). Thus, in this paper the use of non-smooth Newton methods is extended to the case of unilateral frictional wearing contact between an *elastic-damageable* body and a rigid obstacle. By using this model, it is possible to study how initiation of damage depends on fretting wear conditions. A recent numerical approach for simulating fretting wear is presented by Lee et al. (2009). The approach is developed in order to simulate fretting wear of tube-to-plate contacts. In another recent work by Lee et al. (2006) three-dimensional fretting wear was investigated by using finite element analysis. Their results were in good agreement with the results presented by Strömberg (1999). Another recent work on the finite element analysis of fretting wear can be found in Tobi et al. (2009). They present how yielding promotes wear by using a plasticity model with kinematic hardening.

The formulation of the discrete frictional contact problem used here and in the above mentioned references is much based on the papers by Alart and Curnier (1991) and Klarbring (1992). Alart and Curnier derived a mixed formulation of the elastic frictional contact problem as a system of non-smooth equations from a quasi-augmented Lagrangian. An equivalent system of equations was later derived by Klarbring by means of projections. The later formulation has, among others, the advantage of being directly applicable in an inelastic context like the one involving damage considered here. The formulation of Klarbring was further somewhat simplified by Strömberg (1997) in the sense that the Lipschitz continuity, necessary in order to show convergence of Pang's Newton method could be established more easily. In Alart and Curnier (1991) and Klarbring (1992), this property was obtained by replacing the normal contact force by its equivalent projection when formulating Coulomb's law of friction. Strömberg on the other hand proposed that

this could be obtained more easily by replacing the normal contact force by its positive part. The formulation of Strömberg also includes wear. Alart and Curnier suggested further a generalized Newton method (GNM) to solve the resulting system of non-smooth equations, while here it is solved by Pang's Newton method for B-differentiable¹ equations. Although the two approaches might seem very similar, there are two major differences: (i) in the generalized Newton method of Alart and Curnier (1991), the search direction is generated by using an element of the generalized Jacobian while Pang's Newton method make use of the directional derivative and (ii) in Pang's Newton method global convergence is obtained by an Armijo-Goldstein line search procedure, while the generalized Newton method of Alart and Curnier is undamped.

Besides the direct use of Pang's Newton method to solve the coupled inelastic frictional contact problem involving wear and damage, a method based on iteration between subproblems is investigated. This type of methods is common practice for thermoelastic contact problems, where one easily identifies one essentially mechanical and one essentially thermal subproblems which are solved in an iterative process where the mechanical contact problem is solved for a fixed temperature followed by a solution of the heat conduction problem for the updated displacements and contact forces or vice versa, see e.g. Johansson and Klarbring (1993), Wriggers and Miehe (1994), Ireman et al. (2002) or Keppas et al. (2008). A similar algorithm is proposed for a gradient damage model by Ireman (2005), in this context the subproblems consists of an elastic prediction followed by a damage correction. In all these cases this decoupled approach can be seen as a one-step non-linear Gauss-Seidel scheme. A similar splitting strategy has been applied to a dual formulation of the elastic frictional contact problem by Bisenga et al. (2001) and Haslinger et al. (2002). In this case the subproblems consists of a friction problem with given normal forces followed by a contact problem with given tangential forces or vice versa.

This study is organized as follows: In section 2 the governing equations of the model of damage coupled to wear is reviewed. In section 3 the governing equation are put together to form an initial boundary value problem, which is given a formal variational formulation. The problem is discretized by introducing finite element approximations and by replacing time derivatives by Euler-backward differences. Furthermore, the variational inequalities corresponding to Signorini's contact conditions, Coulomb's law of friction and the damage criterion is restated as equivalent equations by means of projections. The result is a system of semi-smooth equations. In section 4 two different algorithms for treating the resulting system

¹ A function is said to be Boulligand-differentiable, or shortly B-differetiable, if it is everywhere directionally differentiable and locally Lipschitz continuous

of discrete equations are presented. The first algorithm is the direct application of Pang’s Newton method, while in the second algorithm the elastic-contact problem is solved for fixed damage followed by the solution of the damage evolution problem for updated displacements and contact forces in an iterative process. In this case Pang’s Newton method is used to solve the semi-smooth subproblems at each step. In section 5 several two-dimensional examples are defined and solved. The performance of the algorithms as well as the behavior of the model is discussed.

2 The model

In this section the governing equations of a model of damage coupled to wear are derived. The presentation complements that in Ireman et al. (2003), where an alternative derivation was presented, as discussed in the Introduction. The governing equations are (i), for the bulk of the body, the equilibrium equations and the constitutive relations of a simple model of isotropic gradient damage coupled to linear elasticity, and (ii), for the contact interface, Signorini’s contact conditions, Coulomb’s law of friction and Archard’s law of wear. In addition the evolution of damage is coupled to the evolution of wear through the boundary conditions of the damage evolution equation.

2.1 General equations

Let us consider a body Ω in a two or three dimensional space, see Figure 1. The state of the body is defined by four state variables $(u, \alpha, u_t^i, \omega)$, which measure the displacement, the damage, the slip and the wear gap, respectively. A superimposed dot denotes a time derivative. Thus, the velocities associated to the state variables are $(\dot{u}, \dot{\alpha}, \dot{u}_t^i, \dot{\omega})$. Furthermore, the corresponding virtual velocities are denoted $(\hat{u}, \hat{\alpha}, \hat{u}_t^i, \hat{\omega})$. The body is subjected to prescribed tractions t on Γ_t , the displacements are fixed on Γ_u and unilateral contact might be developed on Γ_c , as well as friction and wear.

The balance equations of the system is represented by the principle of virtual power which, for quasi-static evolutions, reads

$$\boxed{\hat{\mathcal{P}}_i + \hat{\mathcal{P}}_e = 0} \quad \forall (\hat{u}, \hat{\alpha}, \hat{u}_t^i, \hat{\omega}) \in \mathcal{V} \quad \forall \mathcal{D} \subset \Omega, \tag{1}$$

where \mathcal{V} is a set of admissible virtual velocity fields. In (1) the virtual power of the external forces is given by

$$\hat{\mathcal{P}}_e = \int_{\partial \mathcal{D} \setminus \Gamma_c} t \cdot \hat{u} \, dA, \tag{2}$$

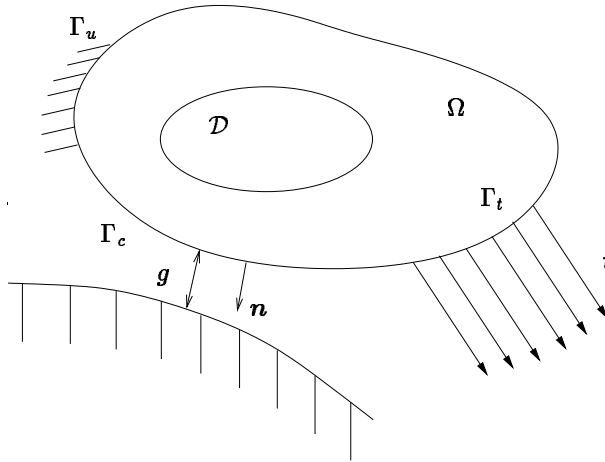


Figure 1: A body Ω unilaterally constrained by a rigid support.

and the virtual power of internal forces is defined by

$$\begin{aligned} \hat{\mathcal{P}}_i = & - \int_{\mathcal{D}} \boldsymbol{\sigma} : \boldsymbol{\varepsilon}(\hat{u}) \, dV - \int_{\mathcal{D}} (A\hat{\alpha} + H \cdot \nabla \hat{\alpha}) \, dV - \int_{\partial \mathcal{D} \setminus \Gamma_c} p \cdot \hat{u} \, dA - \\ & \int_{\partial \mathcal{D} \setminus \Gamma_c} q_t \cdot \hat{u}_t^i \, dA - \int_{\partial \mathcal{D} \setminus \Gamma_c} \mathcal{W} \hat{\omega} \, dA - \int_{\partial \mathcal{D} \setminus \Gamma_c} \mathcal{A} \hat{\alpha} \, dA, \end{aligned} \quad (3)$$

where

$$\boldsymbol{\varepsilon} = \boldsymbol{\varepsilon}(u) = \frac{1}{2}(\nabla u + \nabla u^T), \quad (4)$$

is the infinitesimal strain tensor, $\boldsymbol{\sigma}$ is the Cauchy stress, p is the contact traction vector (with reversed sign), A and \mathcal{A} are internal forces work conjugate to $\hat{\alpha}$, and H is associated to $\nabla \hat{\alpha}$. Furthermore, forces associated to the frictional slip and the wear rate are also introduced. These are denoted q_t and \mathcal{W} , respectively.

Local balance laws for the forces associated to each state variable are now derived from the principle of virtual power in (1) by using the divergence theorem and the fundamental lemma of variational calculus. We then obtain the classical equilibrium equations associated to u , i.e.

$$\begin{cases} \operatorname{div} \boldsymbol{\sigma} = 0 & \text{in } \mathcal{D}, \\ \boldsymbol{\sigma} n = t & \text{on } \partial \mathcal{D} \setminus \Gamma_c, \\ \boldsymbol{\sigma} n = -p & \text{on } \partial \mathcal{D} \cap \Gamma_c, \end{cases} \quad (5)$$

as well as the following balance equations for forces associated to α :

$$\begin{cases} \operatorname{div} H - A = 0 & \text{in } \mathcal{D}, \\ H \cdot n = -\mathcal{A} & \text{on } \partial \mathcal{D} \cap \Gamma_c, \\ H \cdot n = 0 & \text{on } \partial \mathcal{D} \setminus \Gamma_c, \end{cases} \quad (6)$$

where n is the outward unit normal vector of the boundary of \mathcal{D} . These sets of local balance laws are also found in the formulation of Frémond and Nedjar (1996). However, in the present case we also obtain balance equations associated to u_t^i and ω :

$$\begin{cases} q_t = 0 & \text{on } \partial \mathcal{D} \cap \Gamma_c, \\ \mathcal{W} = 0 & \text{on } \partial \mathcal{D} \cap \Gamma_c. \end{cases} \quad (7)$$

Consequently, the two forces, q_t and \mathcal{W} , are simply equal to zero. However, one might think of phenomena when gradients of u_t^i and ω are included in the definition of the internal virtual power. For instance, if one attempts to develop a theory for wear debris transportation one might use the gradient of the wear rate. It is also possible to involve external forces that drives wear, e.g., of chemical origin. In these cases the balance equations will be nontrivial.

In addition to balance laws we need constitutive assumptions that couple the internal forces to the state variables. A general framework for that is obtained by using free energies and dissipation potentials in the style of a standard material. Such an approach gives equations that satisfy the second law of thermodynamics, which in a purely mechanical setting, as the present one, postulates that the change in total free energy $\dot{\Upsilon}$ must be less than the external power \mathcal{P}_e , i.e.

$$\boxed{\dot{\Upsilon} \leq \mathcal{P}_e} \quad \forall \mathcal{D} \subset \Omega. \quad (8)$$

The internal and external powers \mathcal{P}_i and \mathcal{P}_e are obtained from (2) and (3) by replacing the virtual fields by the corresponding real velocities.

We assume that the total free energy of our system is given by

$$\Upsilon = \int_{\mathcal{D}} \rho \psi \, dV + \int_{\partial \mathcal{D} \cap \Gamma_c} \Psi \, dA, \quad (9)$$

where ρ is the mass density, $\psi = \psi(\varepsilon, \alpha, \nabla \alpha)$ is the local free energy in Ω and $\Psi = \Psi(u_n, u_t, u_t^i, \omega, \alpha)$ is the local free energy on Γ_c . By using (1) and (9) in (8) and localizing, we obtain the following inequalities:

$$\begin{cases} \rho \dot{\psi} \leq \sigma : \varepsilon(\dot{u}) + A \dot{\alpha} + H \cdot \nabla \dot{\alpha} & \text{in } \mathcal{D}, \\ \dot{\Psi} \leq p \cdot \dot{u} + \mathcal{A} \dot{\alpha} + q_t \cdot \dot{u}_t^i + \mathcal{W} \dot{\omega} & \text{on } \partial \mathcal{D} \cap \Gamma_c. \end{cases} \quad (10)$$

The first line of (10) is known as the Clausius-Duhem inequality and the second line is its boundary counterpart. In the following, evolutions that satisfies these inequalities are obtained by introducing state laws and dissipation potentials.

The state laws in Ω , i.e., for the bulk, are

$$\begin{cases} \sigma = \rho \frac{\partial \psi}{\partial \varepsilon}, \\ A^r = \rho \frac{\partial \psi}{\partial \alpha}, \\ H = \rho \frac{\partial \psi}{\partial (\nabla \alpha)}, \\ A^i = A - A^r. \end{cases} \quad (11)$$

Taking the time derivative of ψ , multiplying by ρ and inserting the state laws above gives

$$\rho \dot{\psi} = \sigma : \varepsilon(\dot{u}) + (A - A^i)\dot{\alpha} + H \cdot \nabla \dot{\alpha}. \quad (12)$$

The Clausius-Duhem inequality (10)₁ and (12) give

$$A^i \dot{\alpha} \geq 0 \quad \text{in } \mathcal{D}. \quad (13)$$

This is the local dissipation inequality in Ω , which we satisfy by introducing a dissipation potential $\phi = \phi(A^i; \varepsilon, \alpha)$ defined on Ω . It is convex with respect to A^i and satisfies

$$\begin{cases} \phi(0; \varepsilon, \alpha) = 0, \\ 0 \in \partial(0; \varepsilon, \alpha). \end{cases} \quad (14)$$

Here, and in the following, ∂ denotes sub-differential with respect to the arguments before ‘;’. The reason for using a sub-differential instead of a standard derivative is that the studied phenomena are non-smooth. Based on the dissipation potential we now assume the following (complementary) constitutive law:

$$\dot{\alpha} \in \partial \phi(A^i; \varepsilon, \alpha). \quad (15)$$

It is straight forward to prove that (15) implies satisfaction of the dissipation inequality in (13).

As state laws for the contact interface we assume

$$\begin{cases} (p_n, p_t, q_t^r, \mathcal{W}^r, \mathcal{A}^r) \in \partial \Psi, \\ q_t^i = q_t - q_t^r, \\ \mathcal{W}^i = \mathcal{W} - \mathcal{W}^r, \\ \mathcal{A}^i = \mathcal{A} - \mathcal{A}^r. \end{cases} \quad (16)$$

By using the definition of the sub-differential and a treatment of the time derivative as the left-hand derivative, one can derive the following inequality:

$$\dot{\Psi} \geq p_n \dot{u}_n + p_t \dot{u}_t - q_t^i \cdot \dot{u}_t^i + (\mathcal{A} - \mathcal{A}^i) \dot{\alpha} - \mathcal{W}^i \dot{\omega}. \quad (17)$$

This is shown in detail Ireman et al. (2003). In (16) and (17) we have used the following decomposition of p and u into normal components and tangential vectors:

$$p_n = p \cdot n, p_t = (I - n \otimes n)p, u_n = u \cdot n, u_t = (I - n \otimes n)u,$$

where I is the second order identity tensor and \otimes denotes the tensor product of two vectors. Introducing (17) in (10) results in

$$q_t^i \cdot \dot{u}_t^i + \mathcal{A}^i \dot{\alpha} + \mathcal{W}^i \dot{\omega} \geq 0 \quad \text{on } \partial \mathcal{D} \cap \Gamma_c, \quad (18)$$

which is the local dissipation inequality on Γ_c . This inequality is satisfied by introducing a dissipation potential $\Phi = \Phi(q_t^i, \mathcal{A}^i, \mathcal{W}^i; p_n, \omega, \alpha)$, which is convex with respect to first three arguments and satisfies

$$\begin{cases} \Phi(0, 0, 0; p_n, \omega, \alpha) = 0, \\ (0, 0, 0) \in \partial \Phi(0, 0, 0; p_n, \omega, \alpha). \end{cases} \quad (19)$$

The complementary constitutive laws for the interface are now given by

$$(\dot{u}_t^i, \dot{\alpha}, \dot{\omega}) \in \partial \Phi(q_t^i, \mathcal{A}^i, \mathcal{W}^i; p_n, \omega, \alpha), \quad (20)$$

which are such that the dissipation inequality in (10)₂ is satisfied.

2.2 Fretting fatigue model

The general model of the previous subsection is now given particular form by picking explicit free energies and dissipation potentials. For the bulk we use those of Frémond and Nedjar (1996), which read as follows:

$$\begin{cases} \psi = \frac{1}{2\rho} ((1 - \alpha)(\lambda \text{tr}(\varepsilon)^2 + 2G\varepsilon : \varepsilon) + c(\nabla \alpha)^2), \\ \phi(A^i; \varepsilon, \alpha) = I_{\mathcal{B}(\varepsilon, \alpha)}(A^i), \\ \mathcal{B}(\varepsilon, \alpha) = \{A : A - \frac{1}{2}\alpha(\lambda \text{tr}(\varepsilon)^2 + 2G\varepsilon : \varepsilon) - W \leq 0\}. \end{cases} \quad (21)$$

Actually this is a slight simplification of the model of Frémond and Nedjar (1996) since we do not include any difference in behavior in tension and compression. In (21), λ and G are Lamé's coefficients, c is a parameter which influence the size of the damage zone,

$$I_K(x) = \begin{cases} 0 & x \in K \\ \infty & x \notin K \end{cases}$$

is the indicator function of a convex set K and W is a threshold on the strain energy for initiation of damage. Note that we expect that $\alpha \in [0, 1]$, where $\alpha = 0$ corresponds to undamaged material and $\alpha = 1$ to completely damaged material. However, as discussed in Ireman et al. (2003), we do not need to treat this constraint explicitly since $\dot{\alpha} \rightarrow 0$ as $\alpha \rightarrow 1$ and the lower bound is satisfied due to the specific form of the dissipation function. Using (21) in (11) together with the balance laws in (6) yields

$$\begin{cases} \sigma = (1 - \alpha)(\lambda \text{tr}(\varepsilon)I + 2G\varepsilon), \\ A^r = -\frac{1}{2}(\lambda \text{tr}(\varepsilon)^2 + 2G\varepsilon : \varepsilon), \\ H = c\nabla\alpha, \\ A^i = c\Delta\alpha + \frac{1}{2}(\lambda \text{tr}(\varepsilon)^2 + 2G\varepsilon : \varepsilon), \end{cases} \quad (22)$$

where Δ denotes the Laplace operator. Furthermore, (21) in (15), using (6) and (22), yields

$$\begin{cases} \dot{\alpha} \geq 0, \quad R \leq 0, \quad \dot{\alpha}R = 0, \\ R = c\Delta\alpha + \frac{1}{2}(1 - \alpha)(\lambda \text{tr}(\varepsilon)^2 + 2G\varepsilon : \varepsilon) - W. \end{cases} \quad (23)$$

Next, we suggest explicit relationships for the free energy and the dissipation potential on the contact interface. These are

$$\begin{cases} \Psi = I_C(u_n, \omega) + I_D(u_t, u_t^i) + \frac{1}{2}(1 - \alpha)^2 \kappa \omega, \\ \Phi = I_{\mathcal{F}(p_n, \alpha)}(q_t^i, \mathcal{W}^i) + I_{\mathcal{G}}(\mathcal{A}^i), \\ C = \{(u_n, \omega) : u_n - \omega - g \leq 0\}, \\ D = \{(u_t, u_t^i) : u_t - u_t^i = 0\}, \\ \mathcal{F}(p_n, \alpha) = \{(q_t, \mathcal{W}) : |q_t| + k\mathcal{W} p_n \leq (p_n)_+ + k(p_n - \frac{1}{2}(1 - \alpha)^2)p_n\}, \\ \mathcal{G} = \{\mathcal{A} : \mathcal{A} = 0\}. \end{cases} \quad (24)$$

Three constitutive parameters appear in these expression. Two of them are well-known: the coefficient of friction μ and the wear coefficient k . The third parameter, denoted κ , represents how wear influences damage on the contact surface. By inserting (24) in (16) and utilizing the trivial balance laws in (7), one obtains

$$\begin{cases} p_n \geq 0, \quad u_n - \omega - g \leq 0, \quad p_n(u_n - \omega - g) = 0, \\ \mathcal{W}^r = -p_n, \quad q_t^r = -p_t, \quad \mathcal{A}^r = -(1 - \alpha)\kappa\omega, \\ q_t^i = p_t, \\ \mathcal{W}^i = p_n, \\ \mathcal{A}^i = (1 - \alpha)\kappa\omega - c\nabla\alpha \cdot n. \end{cases} \quad (25)$$

From the first of these conditions, which is a generalization of Signorini’s contact conditions, it is clear that g can be interpreted as an initial gap between the body and the obstacle, as shown in Figure 1, and $\omega + g$ is the undeformed gap after wear has occurred. One may also note that (25) identifies the forces q_t^i and \mathcal{W}^i as being equal to tangential and normal traction components. Finally, (24) in (20) together with (25) gives

$$\begin{cases} |\dot{u}_t| p_t = \dot{u}_t \mu(p_n)_+, & |p_t| \leq \mu(p_n)_+, \\ \dot{\omega} = k p_n |\dot{u}_t|, \\ \mathcal{A}^i = 0, & \dot{\alpha} \in \mathbb{R}. \end{cases} \quad (26)$$

The first line of (26) is Coulumb’s law of friction, the second is Archard’s law of wear and the third, together with the last line of (25) gives the coupling between wear and damage.

2.3 Summary of governing equations

Summarizing, the elastic-damage behavior of the body is governed by the following constitutive relations:

$$\sigma = (1 - \alpha)(\lambda \text{tr}(\varepsilon)I + 2G\varepsilon) \quad \text{in } \Omega, \quad (27)$$

$$c\Delta\alpha + \frac{1}{2}(1 - \alpha)(\lambda \text{tr}(\varepsilon)^2 + 2G\varepsilon : \varepsilon) - W + R = 0 \quad \text{in } \Omega, \quad (28)$$

$$\dot{\alpha} \geq 0, \quad R \geq 0, \quad R\dot{\alpha} = 0 \quad \text{in } \Omega, \quad (29)$$

$$n \cdot c\nabla\alpha = 0 \quad \text{on } \partial\Omega \setminus \Gamma_c. \quad (30)$$

An experimental procedure for determining the parameters in these relations is proposed in Frémond and Nedjar (1996). The strain energy threshold W can be determined from a traction test, where it corresponds to the strain energy when the stress-strain curve deviates from the linear elastic one. Furthermore, the parameter c can be related to the size of the damaged zone observed e.g. in a three point bending test of a notched specimen.

At the contact interface Signorini’s contact conditions, Coulomb’s law of friction and Archard’s law of wear have been derived. In addition it has been found that wear will result in a flux of damage into the body. The constitutive equations of the contact interface can be summarized as:

$$p_n \geq 0, \quad u_n - \omega - g \leq 0, \quad p_n(u_n - \omega - g) = 0 \quad \text{on } \Gamma_c, \quad (31)$$

$$|\dot{u}_t| p_t = \mu(p_n)_+, \quad |p_t| \leq \mu(p_n)_+ \quad \text{on } \Gamma_c, \quad (32)$$

$$\dot{\omega} = k(p_n)_+ |\dot{u}_t| \quad \text{on } \Gamma_c, \quad (33)$$

$$n \cdot c\nabla\alpha = (1 - \alpha)\kappa\omega \quad \text{on } \Gamma_c. \quad (34)$$

Equation (34) states that the influx of damage is proportional to the amount of wear, which in turn measures the amount of accumulated slip. Thus, this coupling represents the fact that the damage resistance is decreased depending on the accumulated slip. The factor $(1 - \alpha)$ ensures that an already completely damaged material cannot be further damaged by influx of damage at the boundary. The determination and validity of the local coefficients of friction and wear as indicated by the equations (32) and (33) in a fretting context are discussed by McColl et al. (2004). They conclude that the coefficient of friction taken as the stabilized value obtained from a fretting wear test and the wear coefficient taken as an average obtained from a measured wear profile gives good agreement between simulation and experimental results. Finally, provided that all parameters are known for the bulk material, the coupling parameter could be determined by examining the damaged zone under the contact and comparing it to the damage calculated without coupling.

If the information on the additional parameters c and κ is not available one can always choose $\kappa = 0$ and thus treat the problem without explicit coupling between damage and wear and regard c as a smoothing parameter to be adjusted in the subsequent numerical procedure.

3 The system of discrete equations

In this section a discrete system of equations are derived from the governing equations presented above. The derivation may be outlined as follows: (i) weak forms of the governing equations are introduced and put together to form an initial boundary value problem, where the complementarity conditions of the damage evolution law, Signorini's contact conditions and Coulomb's law of friction are stated as variational inequalities; (ii) finite element approximations of the displacement- and damage fields are introduced and certain integrals are evaluated using appropriate quadrature rules; (iii) time rates are approximated using Euler-backward differences; (iv) the discrete variational inequalities are restated as equivalent equations by means of projections. The result is a system of semi-smooth equations which is solved in the next section.

3.1 Variational formulation

Here the second variational formulation presented in Ireman et al. (2003) is used since it has been proven to be the most practical (Ireman, 2005). The initial boundary value problem reads: Given proper initial conditions and a load history $t(t)$ on a time interval $[0, \tau]$ find $u : [0, \tau] \rightarrow \mathcal{V}$, $\alpha : [0, \tau] \rightarrow \mathcal{B}$, $R : [0, \tau] \rightarrow \mathcal{R}$, $p_n : [0, \tau] \rightarrow \mathcal{H}_n$ and $p_t : [0, \tau] \rightarrow \mathcal{F}(p_n)$ such that for each time $t \in [0, \tau]$

$$\int_{\Omega} \sigma : \varepsilon(v) dV - \int_{\Gamma_t} t \cdot v dA + \int_{\Gamma_c} p \cdot v dA = 0 \quad \forall v \in \mathcal{V}, \quad (35)$$

$$\int_{\Omega} c \nabla \alpha \cdot \nabla \beta \, dV - \int_{\Omega} R \beta \, dV - \frac{1}{2} \int_{\Omega} (1 - \alpha) (\lambda \operatorname{tr}(\varepsilon)^2 + 2G \varepsilon : \varepsilon) \beta \, dV + \int_{\Omega} W \beta \, dV - \int_{\Gamma_c} (1 - \alpha) \kappa \omega \beta \, dA = 0 \quad \forall \beta \in \mathcal{B}, \quad (36)$$

$$\int_{\Omega} \dot{\alpha} (R - S) \, dV \leq 0 \quad \forall S \in \mathcal{R}, \quad (37)$$

$$\int_{\Gamma_c} (\gamma_n - p_n) (u_n - \omega - g) \, dA \leq 0 \quad \forall \gamma_n \in \mathcal{K}_n, \quad (38)$$

$$\int_{\Gamma_c} (\gamma_t - p_t) \cdot \dot{u}_t \, dA \leq 0 \quad \forall \gamma_t \in \mathcal{F}(p_n), \quad (39)$$

where in addition (27) and (33) hold and the following notations for sets of functions are used:

$$\mathcal{V} = \{v : v(x) = 0, \quad x \in \Gamma_u\},$$

$$\mathcal{R} = \{R : R(x) \geq 0, \quad x \in \Omega\},$$

$$\mathcal{K}_n = \{p_n : p_n(x) \geq 0, \quad x \in \Gamma_c\},$$

$$\mathcal{F}(p_n) = \{p_t : |p_t(x)| \leq \mu(p_n(x))_+, \quad x \in \Gamma_c\}$$

and \mathcal{B} is a set of sufficiently smooth function on Ω . Equation (35) is the weak form of the equilibrium equations (5), equation (36) is the weak form of the damage criterion (28),(30) and (34), the variational inequality (37) is equivalent to the complementarity conditions (29), the variational inequality (38) is equivalent to Signorini's contact conditions (31) and the variational inequality (39) is equivalent to Coulomb's law of friction (32).

3.2 Space discretization

In the following only two-dimensional problems are discussed. The problem stated above is discretized by introducing finite dimensional approximations of the sets of functions and evaluating certain integrals in the variational expressions using appropriate quadrature rules. The extension to three-dimensional problems is straightforward for the variational inequalities (35)-(37) and the derivation, discretization and numerical treatment in a three-dimensional setting of the variational inequalities corresponding to (32) and (33) is found in Strömberg (1999).

In order to simplify the formulation, a global matrix based notation for the shape functions and their derivatives are introduced. A detailed element-wise formulation of the elastic gradient-damage problem is given in Ireman (2005). The displacement- and damage fields are approximated by

$$u(x) = N_u(x)d \quad \text{and} \quad \alpha(x) = N_\alpha(x)q, \quad (40)$$

respectively, where N_u is a matrix of shape functions used to approximate the displacement field, d is the vector of nodal displacements, N_α is a matrix of shape functions used to approximate the damage field and q is the vector of nodal values of damage. The strain and gradient of damage fields are consequently approximated by

$$\varepsilon(x) = B_u(x)d \quad \text{and} \quad \nabla\alpha(x) = B_\alpha(x)q, \tag{41}$$

respectively, where B_u and B_α are matrices containing derivatives of the shape functions used in (40). Furthermore, integrals over Γ_c are evaluated using a quadrature rule of the form

$$\int_{\Gamma_c} f(x) dA \simeq \sum_{M \in \eta_c} f(x^M) I^M, \tag{42}$$

where η_c is the set of integration points on Γ_c and I^M are integration weights. Finally, certain integrals over Ω are evaluated by the same type of rule, i.e.

$$\int_{\Omega} f(x) dV \simeq \sum_{A \in \eta} f(x^A) I^A, \tag{43}$$

where η is the set of integration points in Ω and I^A are integration weights. The integration points are chosen such that the set η_c coincides with the set of nodal points on Γ_c and such that the set η coincides with the set of nodal points in Ω . When bilinear approximations to the displacement and damage fields are used, the trapezoidal rule is chosen in both (42) and (43). For quadratic elements, the corresponding consistent choice is Simpson's rule.

By performing the discretization outlined above one obtains the following discrete equilibrium equations from (35) with (27) inserted:

$$F_i(d, q) + C_n^T P_n + C_t^T P_t - F_e = 0, \tag{44}$$

and the following discrete damage criterion from (36):

$$G(d, q) - DR - \bar{L}(q, \omega) = 0, \tag{45}$$

where

$$F_i(d, q) = \int_{\Omega} (1 - N_\alpha q) B_u^T E B_u d dV,$$

$$C_n = [N_u^T(x^M) n(x^M)],$$

$$C_t = [N_u^T(x^M) n_t(x^M)],$$

$$P_n = \{p_n(x^M)I^M\},$$

$$P_t = \{p_t(x^M)I^M\},$$

$$F_e = \int_{\Gamma_t} N_u^T t \, dA,$$

$$G(d, q) = \int_{\Omega} \left(B_{\alpha}^T E B_{\alpha} q - N_{\alpha}^T \left(\frac{1}{2} (1 - N_{\alpha} q) d^T B_u^T E B_u d - W \right) \right) dV,$$

$$D = [N_{\alpha}^T(x^A)I^A], \quad R = \{R^A\}$$

and

$$\bar{L} = \sum_{M \in \eta_c} N_{\alpha}^T(x^M) (1 - N_{\alpha}(x^M) q) \kappa \omega(x^M) I^M. \quad (46)$$

Furthermore, E is the constitutive matrix of isotropic linear elasticity and n_t is the unit tangent vector of the potential contact surface.

By introducing the approximation (40)₂ into (37) and evaluating the integral by the quadrature rule (43) one finds that the following variational inequality must hold for all nodal points $A \in \eta$:

$$R^A \in \mathcal{R}^h : \quad \dot{q}^A (R^A - S^A) \leq 0 \quad \forall S^A \in \mathcal{R}^h \quad (47)$$

where $\mathcal{R}^h = \{R^A : R^A \geq 0\}$. The details are found in Ireman (2005). In the same way, by inserting the approximation (40)₁ into (38) and (39) and using the quadrature rule (42) one finds that the following variational inequalities must hold for all contact nodes $M \in \eta_c$:

$$P_n^M \in \mathcal{K}_n^h : \quad (Q_n^M - P_n^M)(u_n^M - \omega^M - g^M) \leq 0 \quad \forall Q_n^M \in \mathcal{K}_n^h \quad (48)$$

and

$$P_t^M \in \mathcal{F}^h(P_n^M) : \quad \dot{u}_t^M (Q_t^M - P_t^M) \leq 0 \quad \forall Q_t^M \in \mathcal{F}^h(P_n^M), \quad (49)$$

where $\mathcal{K}_n^h = \{P_n^M : P_n^M \geq 0\}$, $\mathcal{F}^h(P_n^M) = \{P_t^M : |P_t^M| \leq \mu(P_n^M)_+\}$, $\omega^M = \omega(x^M)$, $g^M = g(x^M)$, $\{u_n^M\} = C_n d$ and $\{u_t^M\} = C_t d$. The details are found in Strömberg (1997).

Finally, it is assumed that Archard's law of wear (33) holds at each contact node, i.e.

$$\dot{\omega}^M = \frac{k}{I^M} (P_n^M)_+ |u_t^M|. \quad (50)$$

3.3 Time discretization

The time rates appearing in (47), (49) and (50) are approximated by Euler backward differences, i.e.

$$\dot{q}(t_{k+1}) \simeq \frac{q(t_{k+1}) - q(t_k)}{t_{k+1} - t_k}, \tag{51}$$

$$\dot{u}_t^M(t_{k+1}) \simeq \frac{u_t^M(t_{k+1}) - u_t^M(t_k)}{t_{k+1} - t_k} \tag{52}$$

and

$$\dot{\omega}^M(t_{k+1}) \simeq \frac{\omega^M(t_{k+1}) - \omega^M(t_k)}{t_{k+1} - t_k}. \tag{53}$$

Inserting (51) into (47) gives

$$R^A \in \mathcal{R}^h : \quad \bar{q}^A (R^A - S^A) \leq 0 \quad \forall S^A \in \mathcal{R}^h, \tag{54}$$

where $\bar{q} = q(t_{k+1}) - q(t_k)$. Furthermore, inserting (52) into (49) gives

$$P_t^M \in \mathcal{F}^h(P_n^M) : \quad \bar{u}_t^M (Q_t^M - P_t^M) \leq 0 \quad \forall Q_t^M \in \mathcal{F}^h(P_n^M), \tag{55}$$

where $\bar{u}_t^M = u_t^M(t_{k+1}) - u_t^M(t_k)$. Finally, inserting (52) and (53) into (50) gives

$$\omega^M(t_{k+1}) = \omega_0^M + \frac{k}{I^M} (P_n^M)_+ |\bar{u}_t^M|, \tag{56}$$

where $\omega_0^M = \omega^M(t_k)$. Now ω^M can be eliminated from (46) by inserting (56) resulting in

$$L = \sum_{M \in \eta_c} N_\alpha^T(x^M) (1 - N_\alpha(x^M)q) \kappa (\omega_0^M I^M + k (P_n^M)_+ |\bar{u}_t^M|). \tag{57}$$

3.4 Projections

The last step in obtaining a suitable formulation for the subsequent numerical treatment is to restate the variational inequalities (48), (54) and (55) as equivalent equations by means of projections (Klarbring, 1992). The result is

$$R^A = (R^A - r\bar{q}^A)_+, \tag{58}$$

$$P_n^M = (P_n^M + r(u_n^M - \omega_0^M - \frac{k}{I^M} (P_n^M)_+ |\bar{u}_t^M| - g^M))_+ \tag{59}$$

and

$$P_t^M = \begin{cases} P_t^M + r\bar{u}_t^M & \text{if } |P_t^M + r\bar{u}_t^M| \leq \mu(P_n^M)_+ \\ \mu(P_n^M)_+ \text{sgn}(P_t^M + r\bar{u}_t^M) & \text{otherwise} \end{cases}, \quad (60)$$

where $r > 0$ is a parameter which can be chosen arbitrarily and possibly with different values in (58), (59) and (60), and $(\cdot)_+ = \max(0, \cdot)$ denotes the positive part of a scalar. The details of the derivation of (58) are found in Ireman (2005) and the details for obtaining (59) and (60) are found e.g. in Ireman et al. (2002).

3.5 System of semi-smooth equations

The discrete problem to be solved at each time step is defined by equations (44)-(45) and (58)-(60) and can be summarized as the following set of semi-smooth equations:

$$H(y) = \begin{cases} F_i(d, q) + C_n^T P_n + C_t^T P_t - F_e \\ G(d, q) - DR - L(d, q, P_n) \\ -R + \Pi_q(q, R) \\ -P_n + \Pi_n(d, P_n) \\ -P_t + \Pi_t(d, P_n, P_t) \end{cases} = 0, \quad (61)$$

where $y = (d, q, R, P_n, P_t)$. Here, Π_q , Π_n and Π_t denote the projections defined by (58), (59) and (60), respectively.

Except for the functions L , Π_q , Π_n and Π_t the system of equations (61) is smooth. These functions are however semi-smooth and as such the system of equations can be solved by a modified Newton method suggested by Pang (1990). The method was originally developed for B-differentiable equations, i.e. equations that are directionally differentiable and Lipschitz continuous. A semi-smooth function is essentially a B-differentiable function which has a directional derivative that fulfills an additional requirement. The semi-smoothness of the system of equations implies that the convergence results for the Newton method can be improved (Christensen and Pang, 1998). The semi-smoothness of L , Π_q , Π_n can be established by the same arguments as in Ireman (2005), and the semi-smoothness of Π_t is shown in Christensen and Pang (1998).

4 Algorithms

We investigate the following two approaches for solving $H(y) = 0$: (i) directly using Pang's Newton method for semi-smooth equations and (ii) a decoupled approach based on a Gauss-Seidel scheme where an elastic frictional contact problem

with wear is solved in the first step, followed by the solution of the damage evolution problem with updated displacements and contact forces. In both steps Pang’s Newton method is used to solve the semi-smooth subproblems.

4.1 Pang’s Newton method

The following algorithm for solving a system of semi-smooth equations was suggested by Pang (1990):

Algorithm BN: Let β , γ and ε be given scalars with $\beta \in (0, 1)$, $\gamma \in (0, 1/2)$ and ε small. Repeat the following steps for each time increment $k + 1$:

0. Let y^0 be given from the previous time step k and set $j = 0$.

1. Find a search direction z such that

$$H(y^j) + H'(y^j; z) = 0, \tag{62}$$

where $H'(y^j; z)$ is the directional derivative.

2. Let $\alpha^j = \beta^{m_j}$, where m_j is the smallest integer $m \geq 0$ for which the following decrease criterion holds:

$$\phi(y^j + \beta^m z) \leq (1 - 2\gamma\beta^m)\phi(y^j), \quad \phi(y) = \frac{1}{2}H^T(y)H(y).$$

3. Set $y^{j+1} = y^j + \alpha^j z$.

4. If $\phi(y^{j+1}) \leq \varepsilon$, then terminate with y^{j+1} as an approximate zero of $H(y)$. Otherwise, replace j by $j + 1$ and return to step 1.

Pang’s Newton method with some modifications to be presented is referred to as the Modified Boulligand Newton method (MBN). The system of equations to be solved in (62) is non-linear due to the non-linearity of the directional derivative at non-smooth points. In order to increase the efficiency of solving this step, the directional derivative of these parts is replaced by “approximations” chosen such that the Newton equation (62) becomes linear also at non-differentiable points. At points where $H(y)$ is smooth, the directional derivative is of course linear as $H'(y; z) = \nabla H(y)z$. At non-differentiable points the directional derivative is modified by choosing the directional derivative in one possible direction, say \bar{z} , and defining $J(y)$ by $J(y)\bar{z} = H'(y; \bar{z})$. The directional derivative in all the other directions is then replaced by $H'(y; z) = J(y)z$. Since after such a modification the search direction no longer can be guaranteed to be a descent direction, an upper bound \bar{m}

on m_j in step 2 is introduced in order to prevent the algorithm from stalling. These modifications are crucial for the numerical treatment and were first suggested in Strömberg (1997).

4.2 Directional derivatives

The functions F_i and G are smooth and their directional derivatives are given by

$$F'_i(d, q; z_d, z_q) = \int_{\Omega} (1 - N_{\alpha} q) B_u^T E B_u dV z_d - \int_{\Omega} N_{\alpha} B_u^T E B_u dV z_q \quad (63)$$

and

$$G(d, q; z_d, z_q, z_R) = - \int_{\Omega} N_{\alpha}^T (1 - N_{\alpha} q) d^T B_u^T E B_u dV z_d + \int_{\Omega} (B_{\alpha}^T c B_{\alpha} - N_{\alpha}^T \frac{1}{2} d^T B_u^T E B_u d N_{\alpha}) dV z_q, \quad (64)$$

respectively. Furthermore, as outlined above, the following modified directional derivatives are chosen to replace the actual directional derivatives of the non-smooth functions L , Π_q , Π_n , and Π_t :

$$L'(d, q, P_n; z_d, z_q, z_n) \simeq - \sum_{M \in \eta} N_{\alpha}^T(x^M) N_{\alpha}(x^M) \kappa (\omega_0^M I^M + k(P_n^M)_+ |\bar{u}_t|) z_q + \sum_{M \in \eta_{c1}} N_{\alpha}^T(x^M) (1 - N_{\alpha}(x^M) q) \kappa k (P_n^M \operatorname{sgn}(\bar{u}_t^M) z_{dt}^M + |\bar{u}_t^M| z_n), \quad (65)$$

$$\Pi'_q(q, R; z_q, z_R) \simeq \left\{ \begin{array}{l} z_R^M + r z_q^M \text{ if } R_M - r \bar{q}_M \geq 0 \\ 0 \text{ otherwise} \end{array} \right\}, \quad (66)$$

$$\Pi'_n(d, P_n; z_d, z_n) \simeq \left\{ \begin{array}{l} 0, \quad M \in \eta_{c2} \\ z_n^M + r z_{un}^M, \quad M \in \eta_{c3} \\ z_n^M + r(z_{un}^M - \frac{k}{\bar{l}^M} |\bar{u}_t^M| z_n^M - \frac{k}{\bar{l}^M} P_n^M \operatorname{sgn}(\bar{u}_t^M) z_{ut}^M), \quad M \in \eta_{c4} \end{array} \right\} \quad (67)$$

and

$$\Pi'_t(d, P_n, P_t; z_d, z_n, z_t) \simeq \left\{ \begin{array}{l} 0, \quad M \in \eta_{c5} \\ z_t^M + r z_{ut}^M, \quad M \in \eta_{c6} \\ \mu z_n^M \operatorname{sgn}(P_t^M + r \bar{w}_t^M), \quad M \in \eta_{c7} \end{array} \right\}, \quad (68)$$

respectively, where

$$\begin{aligned} \eta_{c1} &= \{M : P_n^M |u_t^M| > 0\}, \\ \eta_{c2} &= \{M : P_n^M + r(u_n^M - \omega_0^M - \frac{k}{I^M}(P_n^M)_+ |\bar{u}_t^M| - g^M) \leq 0\}, \\ \eta_{c3} &= \{M : P_n^M |\bar{u}_t^M| \leq 0, P_n^M + r(u_n^M - \omega_0^M - \frac{k}{I^M}(P_n^M)_+ |\bar{u}_t^M| - g^M) > 0\}, \\ \eta_{c4} &= \{M : P_n^M |\bar{u}_t^M| > 0, P_n^M + r(u_n^M - \omega_0^M - \frac{k}{I^M}(P_n^M)_+ |\bar{u}_t^M| - g^M) > 0\}, \\ \eta_{c5} &= \{M : P_n^M \leq 0\}, \\ \eta_{c6} &= \{M : P_n^M > 0, |P_t^M + r\bar{u}_t^M| \leq \mu P_n^M\}, \\ \eta_{c7} &= \{M : P_n^M > 0, |P_t^M + r\bar{u}_t^M| > \mu P_n^M\}, \end{aligned}$$

and $z_{un} = C_n z_d$, $z_{ut} = C_t z_d$, $z_n = \{z_n^M\}$ and $z_t = \{z_t^M\}$. These and similar modifications of the directional derivatives have been proven to work well in e.g. Strömberg (1997), Strömberg (1998), Christensen et al. (1998), Strömberg (1999), Christensen (2002a), Christensen (2002b), Ireman et al. (2002) and Ireman (2005).

4.3 Decoupled approach

Instead of solving (61) directly one can adopt an iterative strategy where the contact problem is solved for fixed damage followed by the solution of the damage evolution problem. This strategy has been proven to be successful for a thermo-elastic wear problems (Ireman et al., 2002).

The strategy is applied by first splitting (61) into the following two parts:

$$H_1(y_1, y_2) = \left\{ \begin{array}{l} F_i(d, q) + C_n^T P_n + C_t^T P_t - F_e \\ -P_n + \Pi_n(d, P_n) \\ -P_t + \Pi_t(d, P_n, P_t) \end{array} \right\} = 0$$

and

$$H_2(y_1, y_2) = \left\{ \begin{array}{l} G(d, q) - DR - L(d, q, P_n) \\ -R + \Pi_q(q, R) \end{array} \right\} = 0,$$

where $y_1 = (d, P_n, P_t)$ and $y_2 = (q, R)$. These are then treated by the following algorithm, which can be seen as a non-linear Gauss-Seidel scheme (GS):

Algorithm GS: Repeat the following steps for each time increment $k + 1$:

0. Set $y_2^{i=0} = y_2(t_k)$
1. Solve $\tilde{H}_1(y_1^{i+1}) = H_1(y_1^{i+1}, y_2^i) = 0$ to get y_1^{i+1} .
2. Solve $\tilde{H}_2(y_2^{i+1}) = H_2(y_1^{i+1}, y_2^{i+1}) = 0$ to get y_2^{i+1} .

3. Terminate if $\frac{1}{2}H^T(y^{i+1})H(y^{i+1}) \leq \varepsilon$. Otherwise replace i by $i + 1$ and return to step 1.

When the Gauss-Seidel scheme is applied to the discrete contact-damage problem stated above each of the systems of equations $\tilde{H}_1(y_1^{i+1}) = 0$ and $\tilde{H}_2(y_2^{i+1}) = 0$ are solved by algorithm MBN.

5 Numerical tests

The algorithms presented above are implemented in Matlab 6.1. The problems are scaled such that length unit [mm] are used everywhere, Furthermore, $r = 10^2$ is used in the projection (58) and $r = 10^3$ are used in the projections (59) and (60). In general, these parameters can be chosen in the range between $10^6 I^{-1}$ and $10^9 I^{-1}$, where I is the integration weights in (42) and (43), respectively. Choosing r too small might lead to convergence problems and a too large value might lead to the algorithm stalling. The parameters β , γ and \bar{m} appearing in algorithm MBN are set to $\beta = 0.9$, $\gamma = 0.1$ and $\bar{m} = 22$. This set of parameters was suggested by Strömberg (1997) and has been proven to work well for a large number of problems. Furthermore, observe that

$$\frac{1}{2}H(y)^T H(y) \leq \varepsilon$$

is used as stopping criterion in both algorithms, where ε is set to 10^{-10} .

In this section three example problems are defined and solved. The examples are referred to as Example 1, Example 2 and Example 3, respectively. Results from numerical tests are presented and discussed. These show the lack of mesh dependency, the performance of the algorithms and the behaviour of the model.

5.1 Three examples

In all three examples plain strain is assumed and the bulk properties are chosen to be $E = 35000$ [MPa], $\nu = 0.18$, $c = 0.01$ [N] and $W = 10^{-4}$ [MPa]. These are values representative for concrete found in Nedjar (2001).

The wear coefficient $k=0.1$ [mm²/N] used in the computations is about 1000 times greater than the value observed in many practical situations. This means that one might assume that the results represents about 1000 times the number of cycles that is indicated.

In **Example 1** an elastic-damaging body indented by a rigid punch as shown in figure 2 is considered. The dimensions of the foundation is 200×25 [mm²] and the width of the punch is 100 [mm]. This is also the length of the potential contact

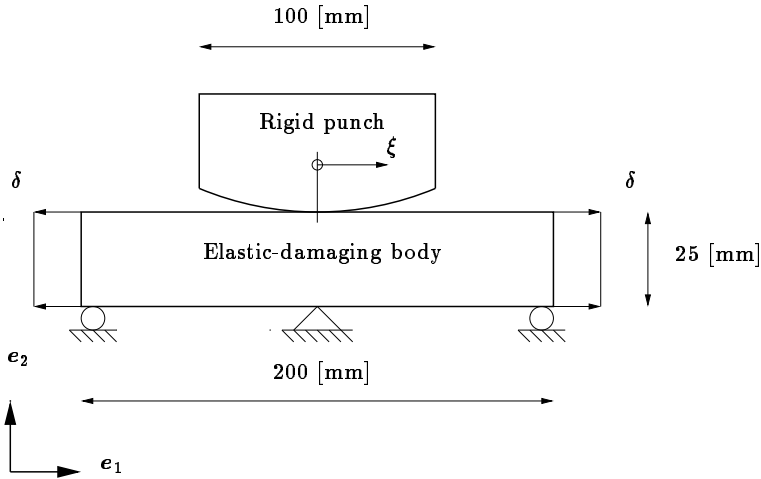


Figure 2: Geometry and boundary conditions for Example 1.

surface defined by the lower end of the punch. The contact gap is described by $g = g_0 \xi^n - g_1$, where g_0 is the maximum indentation depth, g_1 is the actual indentation: $0 \leq g_1 \leq g_0$, ξ is a coordinate along the contact surface chosen such that the edges of the contact surface are at $\xi = -1$ and $\xi = 1$, respectively, and n is either equal to 2 or 4. Furthermore, the sides of the foundation is subjected to prescribed displacements δe_1 on the right-hand side and $-\delta e_1$ on the left hand side. The problem is controlled by controlling the indentation g_1 and the magnitude of the prescribed displacement δ . Two load cases are considered: (i) monotonic loading : the foundation is loaded by first indenting the punch by letting g_1 increase from 0 to $g_0 = 1.5 \cdot 10^{-3}$ [mm] in four time steps and thereafter δ is increased from 0 to $6 \cdot 10^{-3}$ [mm] in the following four time steps and (ii) cyclic loading: the foundation is loaded by first increasing g_1 from 0 to $g_0 = 1.5 \cdot 10^{-3}$ [mm] in four time steps and then the sides of the foundation is subjected to a cyclic prescribed displacement such that δ varies linearly between 0 and $5.5 \cdot 10^{-3}$ [mm]. The purpose of the first load case is to study how the damage depends on the contact geometry and on the coefficient of friction. The purpose of the second load case is to investigate how wear influence on the initiation of damage.

In **Example 2** the lug in figure 3 is considered, where $a = 50$ [mm]. The potential contact interface is defined by the edge of the circular hole. The rigid plug is fixed in space and the gap is $g = 0$ everywhere. The lug is loaded by prescribing the displacement of the lower edge to δe_2 and in order to prevent a rigid body rotation of the lug, the midpoint of the lower edge is also locked in the e_1 -direction. Like in the preceding example, two load cases are considered: (i) monotonic loading, with

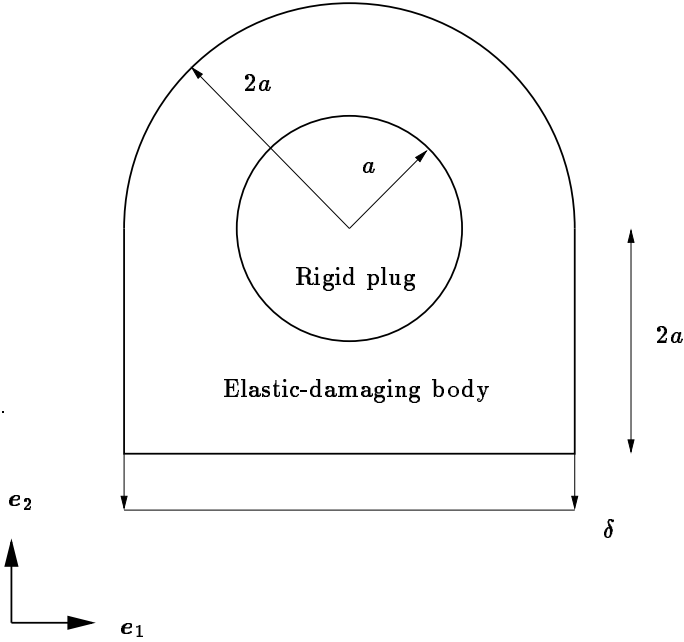


Figure 3: Geometry and boundary conditions for Example 2.

different values of the coefficient of friction, where $\delta = 10^{-2}$ [mm], applied in 20 increments and (ii) cyclic loading, in order to investigate the influence of wear, where δ varies linearly between 0 and $0.5 \cdot 10^{-3}$ [mm] and each cycle is divided into 8 increments.

Finally, in **Example 3** a dovetail joint is considered. The geometry and the boundary conditions are defined in figure 4, where $a = 25$ [mm]. The contact boundary is defined by the figure and the gap is set to $g = 2 \cdot 10^{-3}$ [mm] everywhere. The joint is loaded by a prescribed displacement δe_2 along the upper edge and the mid-point node of the lower edge is locked in the e_1 direction in order to prevent a rigid body rotation. As for the other two examples, a monotonic and a cyclic load case, respectively, are considered. In the monotonic case, a prescribed displacement $1.3 \cdot 10^{-2} e_2$ [mm] is applied in 20 increments. Finally, in the case of cyclic loading a static displacement $0.85 \cdot 10^{-2} e_2$ is combined with a prescribed displacement $\delta_2 e_1$ with δ_2 varying linearly between $0.25 \cdot 10^2$ and $-0.25 \cdot 10^2$. Each cycle is divided into 4 increments.

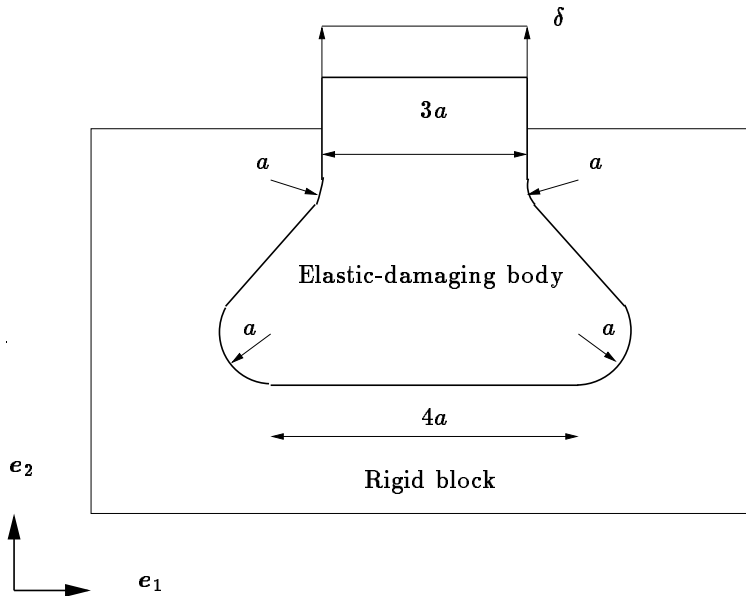


Figure 4: Geometry and boundary conditions for Example 3.

5.2 Solutions for different meshes

Solutions for different refinement of the finite element mesh for example 1, using $n = 4$ and $\mu = 0.5$ are shown in figure 5. In the coarsest mesh, 20 by 3 bilinear elements are used and the potential contact surface is divided into 10 contact elements such that the contact nodes and the displacement nodes coincides as described in the previous sections. The medium mesh consists of 30 by 5 bilinear elements and the contact surface is divided into 20 contact elements. Finally, the most refined mesh is composed by 50 by 10 bilinear elements and 40 contact elements. It is seen that the general appearance of the damage field does not change due to mesh refinement as should be expected from a viable numerical scheme.

5.3 Comparison of the algorithms

We like to compare the performance of the algorithms for the solution of example 1. Cyclic loading with the fourth order punch ($n = 4$), $\mu = 0.5$ and three different combinations of k and κ according to table 1 are considered. The two most refined meshes of figure 5 are used.

Table 2 shows the average values over 100 cycles of the number of Gauss-Seidel iterations per time increment (GS), the total number of Newton iterations per in-

Table 1: Setting of the different test examples.

<i>Set</i>	k [mm ² /N]	κ [MPa]
1	0	0
2	0.1	0
3	0.1	1

crement used to solve subproblem 1 (New1), the total number of line searches per time increment in subproblem 1 (Arm1), the total number of Newton iterations per increment used to solve subproblem 2 (New2), the total number of line searches per time increment in subproblem 1 (Arm1) and the measured CPU time (CPU) per time increment. Furthermore, an 'r' in the Ex-column indicates the most refined mesh and MBN and GS in the Alg.-column refers to direct application of the Newton method and decoupled approach, respectively.

Table 2: Execution statistics for the different algorithms and different settings.

<i>Set</i>	<i>Alg.</i>	<i>GS</i>	<i>New1.</i>	<i>Arm1.</i>	<i>New2.</i>	<i>Arm2.</i>	<i>CPU</i>
1	MBN	-	3.38	3.38	-	-	1.35
	GS	2.38	3.63	3.63	2.63	2.63	1.56
1r	MBN	-	3.50	3.50	-	-	9.53
	GS	2.50	4.63	4.63	3.13	3.13	10.47
2	MBN	-	3.87	9.44	-	-	1.60
	GS	1.60	4.13	10.50	1.79	4.51	1.51
2r	MBN	-	4.69	11.41	-	-	12.37
	GS	2.03	5.66	12.20	2.53	7.75	10.86
3	MBN	-	5.80	37.80	-	-	4.19
	GS	5.17	7.37	13.82	9.56	121.74	5.33
3r	MBN	-	6.19	23.85	-	-	33.77
	GS	5.73	9.09	14.35	12.37	153.05	32.48

Based on these statistics it is difficult to draw a conclusion on which algorithm should be considered as most efficient. There are however some tendencies: Algorithm GS gains efficiency when the number of degrees of freedom is increased. Algorithm MBN seems to always be more efficient for setting 1, i.e. without wear. Algorithm GS seems to always be the most efficient for setting 2 when there is no direct coupling between wear and damage. Finally, for setting 3, the fully coupled problem, the performance is about equal.

5.4 Results for different settings of the examples

The results for the three example problems presented below are obtained using the meshes depicted in figure 6. The geometry of example 1 is approximated using 50 by 10 bilinear elements and 40 contact elements. The lug in example 2 is approximated using 880 bilinear elements and 80 contact elements and finally, the dovetail joint in example 3 is approximated using 960 bilinear elements and 126 contact elements.

Figure 7 shows the calculated damage field for example 1 for different contact geometries and different values of the coefficient of friction. The left-hand figures corresponds to the second order punch ($n = 2$) and the right-hand figures for the fourth order punch ($n = 4$). In all cases the damage will first initiate at the bottom of the foundation, due to the combined effect of the contact load and the bulk load. When there is no friction this damage grows straight up. When there is friction the deformation of the zone right below the contact is restrained and the damage growth is prohibited. Instead damage will initiate at the contact surface close to the edges of the contact near the border between the stick zone and the slip zones. It is also seen that there is more damage at the surface for the fourth order punch than for the second order punch. For $\mu = 0.5$ at the fourth order punch the interior damage and the surface damage is of about the same magnitude.

Figure 8 shows the calculated damage field after 100 cycles for example 1 using different values of k and κ . It is seen that there is very little damage when there is no wear ($\alpha_{max} = 0.05$). If there is wear more damage ($\alpha_{max} = 0.25$) will initiate due to the change of contact geometry. Since wear reduces the contact gap mostly at the edges of the contact, the normal traction will drop there leading to larger deformations of these regions and hence to more damage. Finally, by including the coupling between bulk damage will of course give rise to even more damage at the contact surface ($\alpha_{max} = 0.45$), which in turns weakens the foundation such that damage at the bottom also grows.

Figure 9 shows the calculated damage fields for example 2 for the static load case and different values for the coefficient of friction (to the left) and for the cyclic load case for different values of the wear coefficient and the damage-wear coupling coefficient (to the right).

In this case the coefficient of friction has only a minor influence on the damage since the strain concentration at the centerline of the hole is basically determined by the bulk geometry. For this example, as expected, wear only has no influence on the cyclic behavior, i.e. a deformation that gives rise to no or low damage without wear does not provoke the initiation of damage only due to the slight modification of the contact geometry. On the other hand, the wear coupling will drive the damage at

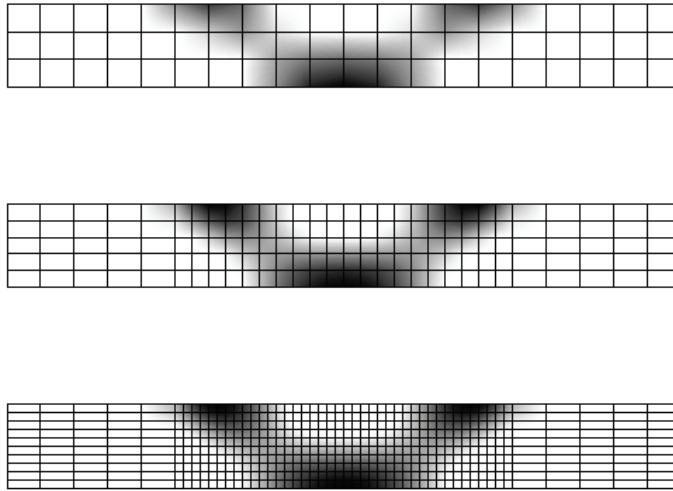


Figure 5: Solutions for example 1, static loading, for different refinements of the mesh.

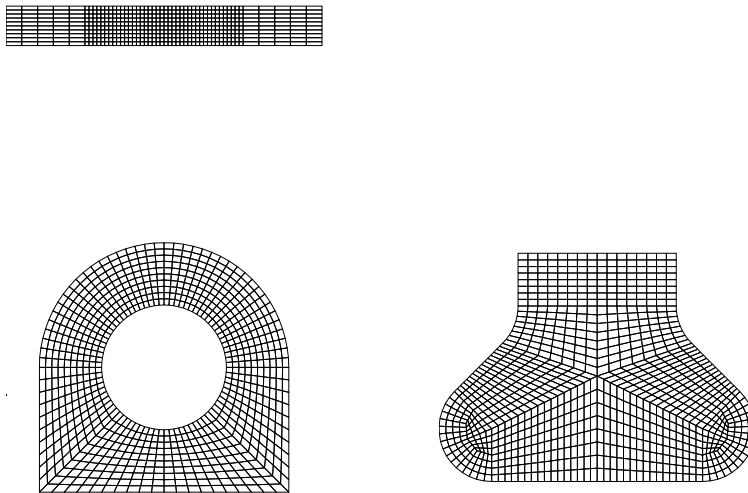


Figure 6: Meshes for the three examples.

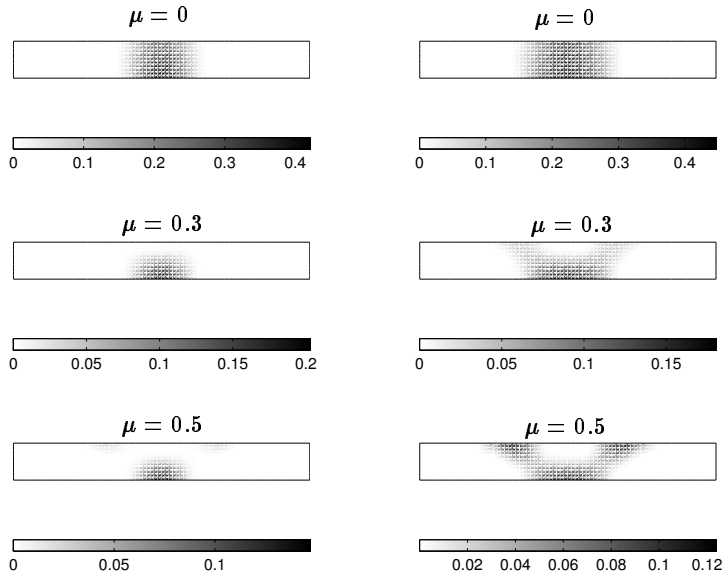


Figure 7: Calculated damage for the static load case of example 1 for a second order punch (the left-hand figures) and a fourth order punch (the right-hand figures), respectively.

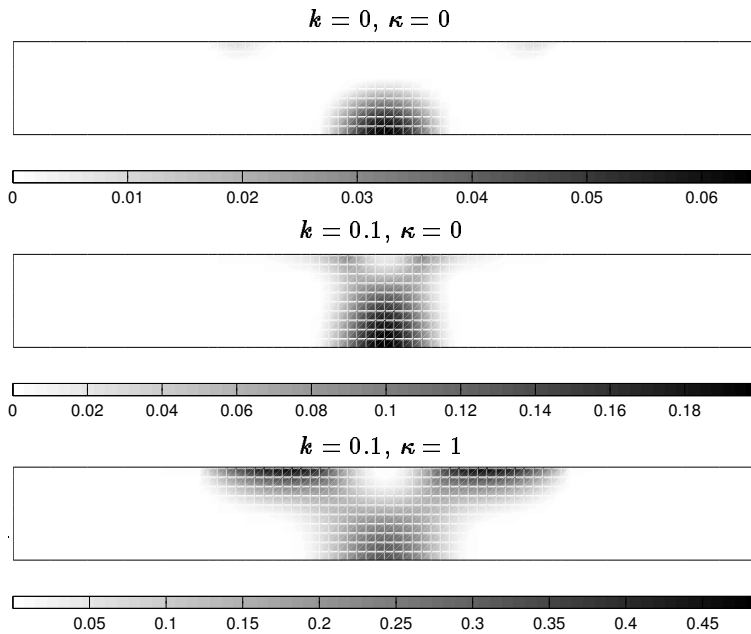


Figure 8: Calculated damage for the cyclic load case of example 1.

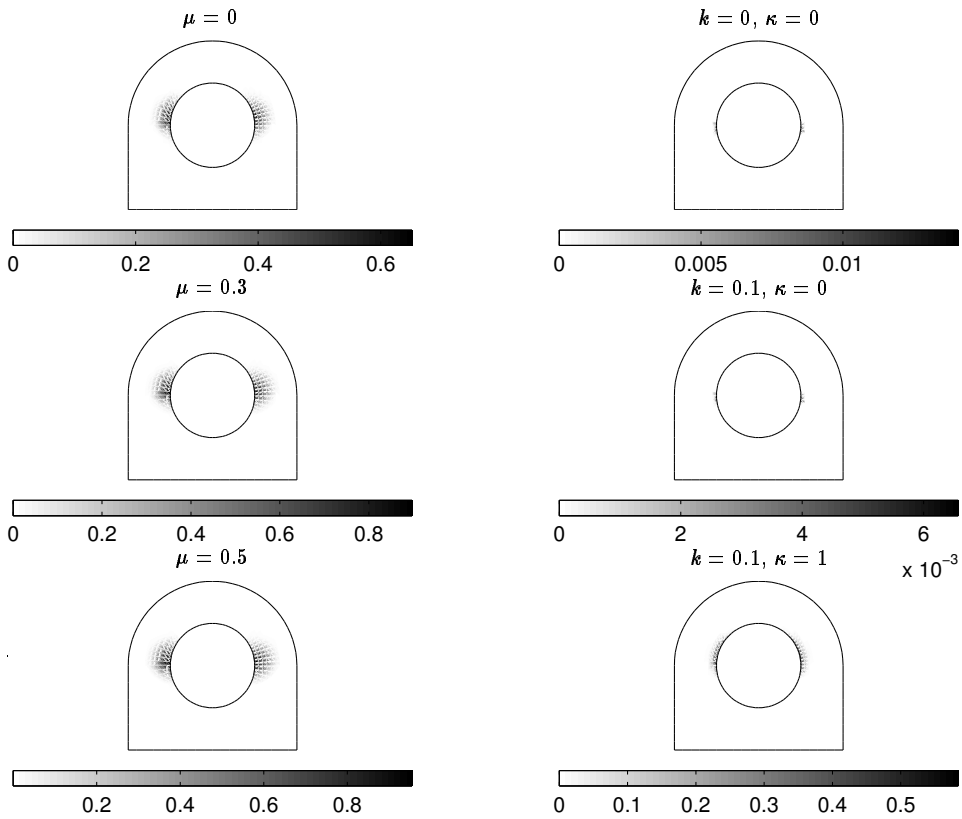


Figure 9: Calculated damage for example 2. In the left column the influence of friction is illustrated and in the right column it is shown how k and κ influence the solution.

the slip zones above the centerline of the whole, but the deformation is insufficient to drive the damage further into the body.

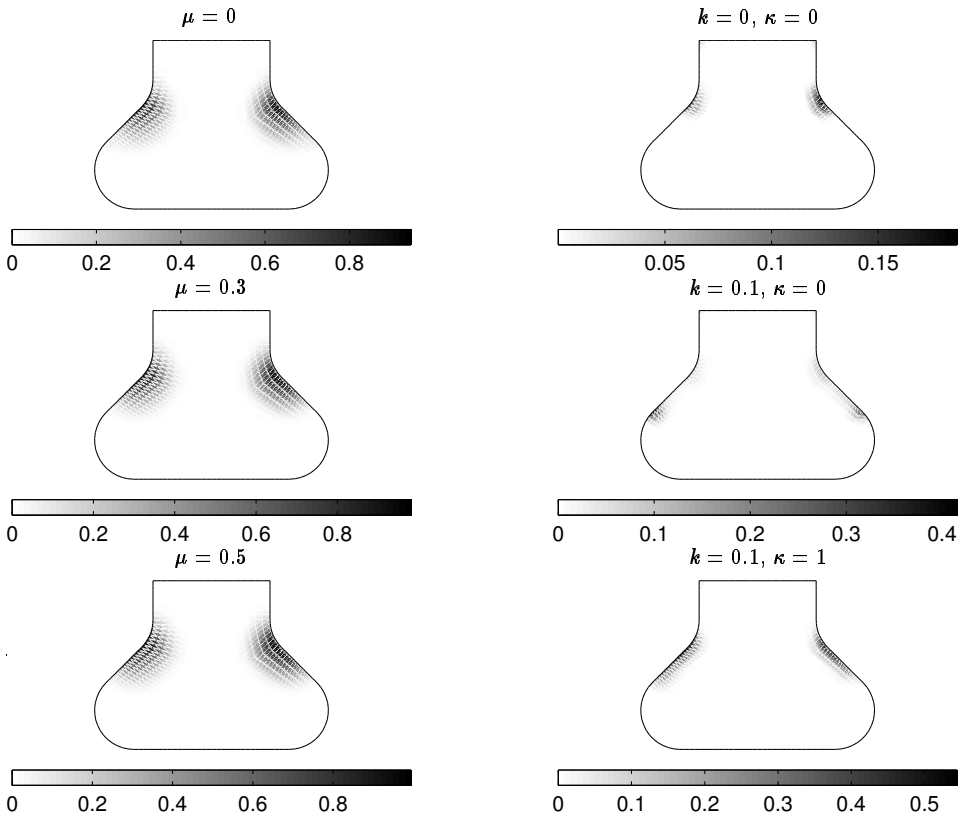


Figure 10: Calculated damage for example 3. In the left column the influence of friction is illustrated and in the right column it is shown how k and κ influence the solution.

The results for example 3, figure 10, shows a similar behaviour as example 2 for static loading (the left-hand figures), i.e. the coefficient of friction has no or a minor influence on the damage field. However, for the cyclic load case (the right-hand figures), this example has the same interesting features as example 1, i.e. a load that gives rise to only minor damage without wear, might give a drastically different result if wear is taken into account even without the explicit coupling between damage and wear.

The solutions to the cyclic load case are slightly asymmetric. This is explained by the fact that the alternating displacement of the top of the body starts to the right ini-

tiating a non symmetric damage field. One would expect to have the mirror image of these solution if the cycle should start to the left instead. This lack of symmetry is kept throughout the load history and the effect is even more pronounced when wear and the wear-damage coupling is present due to the high value of the wear coefficient.

6 Concluding remarks

In the present work a model for numerical studies of fretting fatigue is presented. The model is based on a non-local continuum damage model where coupling to wear is introduced through boundary conditions for the damage field. The model is shown to be consistent with basic postulates of thermodynamics and the framework is general and can be extended in several directions. The numerical treatment of the model is studied in detail and it is shown that the basic numerical issue is the solution of a system of semi-smooth equations. Two approaches for handling these equations are suggested and compared. The first approach is the direct use of a modified Newton method for semi-smooth equations on the fully coupled problem, while in the second approach the elastic wear problem is solved for fixed damage followed by the solution of the damage evolution problem for updated displacements and contact forces, in an iterative process. The latter approach might be viewed as a Gauss-Seidel scheme. When this strategy is used, the modified Newton method is utilized to solve the different subproblems at each Gauss-Seidel step.

It is found that the performance of the algorithms is about equal. It is also shown numerically how the initiation of damage depends on the contact geometry and the coefficient of friction for a monotonically increasing bulk load. Furthermore, it is found that for a cyclic bulk load, damage might initiate spontaneously as a result of the reloading of the contact due to wear. Finally, it is shown how the initiation of damage can be promoted through the coupling to wear.

References

- Alart, P., Curnier, A.** (1991). A mixed formulation for frictional contact problems prone to Newton like solution methods. *Computer Methods in Applied Mechanics and Engineering* **92**, 353-375.
- Bisenga, P., Lebon, F., Maceri, F.** (2001). D-PANA: a convergent block-relaxation solution method for the discretized dual formulation of the Signorini-Coulomb contact problem. *Comptes Rendus de l'Academie de Science Paris, Serie I: Problemes mathématiques de la mécanique* **333**, 1053-1058.

Choon, Y.L., Joon, W.B., Byung, S.C., Young, S.C. (2006). Three dimensional finite element simulation of the fretting wear problems. *International Journal of Modern Physics B* **20**, 3890-3895.

Christensen, P.W., Klarbring, A., Pang, J.S., Strömberg, N. (1998). Formulation and comparison of algorithms for frictional contact problems. *International Journal for Numerical Methods in Engineering* **42**, 145-173.

Christensen, P.W., Pang, J.S. (1998). Frictional contact problems based on semismooth Newton methods. In: Fukushima, M. and Qi, L. (Eds.) *Reformulation - Nonsmooth, Piecewise smooth, Semismooth and Smoothing methods*, Kluwer Academic Publishers, Dordrecht, pp. 81-116.

Christensen, P.W. (2002a). A nonsmooth Newton method for elastoplastic problems. *Computer Methods in Applied Mechanics and Engineering* **191**, 1189-1219.

Christensen, P.W. (2002b). A semi-smooth Newton method for elasto-plastic contact problems. *International Journal of Solids and Structures* **39**, 2323-2341.

Frémond, M. (1987). Adhérence des solides. *Journal de Mécanique théorique et appliquée* **6**, 383-407.

Frémond, M. (1988). Contact with adhesion. In: Moreau, J.J, Panagiotopoulos, P.D. and Strang, G. (Eds.) *Topics in Nonsmooth Mechanics*, Birkäuer Verlag, Basel, pp. 177-221.

Frémond, M., Nedjar, B. (1996). Damage, gradient of damage and principle of virtual power. *International Journal of Solids and Structures* **33**, 1083-1103.

Gurtin, M.E. (2000). *Configurational forces as basic concepts of continuum physics*. Springer-Verlag, New York.

Haslinger, J., Dostál, Z., Kucera, R. (2002). On a splitting type algorithm for the numerical realization of contact problems with Coulomb friction. *Computer Methods in Applied Mechanics and Engineering* **191**, 2261-2281.

Hills, D.A., Nowell, D. (1994). *Mechanics of fretting fatigue*. Kluwer Academic Publications, Dordrecht.

Ireman, P., Klarbring, A., Strömberg, N. (2002). Finite element algorithms for thermoelastic wear problems. *European Journal of Mechanics/A Solids* **21**, 423-440.

Ireman, P., Klarbring, A., Strömberg, N. (2003). A model of damage coupled to wear. *International Journal of Solids and Structures* **40**, 2957-2974.

Ireman, P.J. (2005). Algorithms for gradient-regularized damage models based on a semi-smooth Newton method. *Computer Methods in Applied Mechanics and Engineering*. **194**, 727-741.

Johansson, L., Klarbring, A. (1993). Thermoelastic frictional contact problems: modelling, FE-approximation and numerical realization. *Computer Methods in Applied Mechanics and Engineering* **105**, 181-210.

Johansson, L., Klarbring, A. (2000). Study of frictional impact using a nonsmooth equations solver. *Journal of Applied Mechanics* **67**, 267-273.

Keppas, L.K., Giannopoulos, G.I., Anifantis, N.K. (2008). Transient coupled thermoelastic contact problems incorporating thermal resistance: a BEM approach. *CMES: Computer Modeling in Engineering & Sciences* **25**, 181-196.

Klarbring, A. (1990). Derivation and analysis of rate boundary-value problems of frictional contact. *European Journal of Mechanics, A/Solids* **9**, 53-85.

Klarbring, A. (1992). Mathematical programming and augmented Lagrangian methods for frictional contact problems. In: A Curnier (Ed.), *Proceedings of the Contact Mechanics International Symposium*, 409-422.

Lee C.Y., Tian L.S., Bae J.W., Chai, Y.S. (2009). Application of influence function method on the fretting wear of tube-to-plate contact. *Tribology International* **42**, 951-957.

Maugin, G.A. (1990). Internal variables and dissipative structures. *Journal of Non-Equilibrium Thermodynamics* **15**, 173-192.

McColl, I.R., Ding, J., Leen, S.B. (2004). Finite element simulation and experimental validation of fretting wear. *Wear* **256**, 1114-1127.

Mohd Tobi, A.L., Ding, J., Bandak, G., Leen, S.B., Shipway, P.H. (2009). A study on the interaction between fretting wear and cyclic plasticity for Ti-6Al-4V. *Wear* **267**, 270-282.

Nedjar, B. (2001). Elastoplastic-damage modelling including the gradient of damage: formulation and computational aspects. *International Journal of Solids Structures* **38**, 5421-5451.

Pang, J.S. (1990). Newton's method for B-differentiable equations. *Mathematics of Operations Research* **15**, 311-341.

Raous, M., Canégni, L., Cocu, M. (1999). A consistent model coupling adhesion, friction, and unilateral contact. *Computer Methods in Applied Mechanics and Engineering* **177**, 383-399.

Strömberg, N., Johansson, L., Klarbring, A. (1996). Derivation and analysis of a generalized standard model for contact friction and wear. *International Journal of Solids and Structures* **33**, 1817-1836.

Strömberg, N. (1997). An augmented Lagrangian method for fretting problems. *European Journal of Mechanics, A/Solids* **16**, 573-593.

Strömberg, N. (1998). Finite element treatment of two-dimensional thermoelastic wear problems. *Computer Methods in Applied Mechanics and Engineering* **177**, 441-455.

Strömberg, N. (1999). A Newton method for three-dimensional fretting problems. *International Journal of Solids and Structures* **33**, 2075-2090.

Strömberg, N. (2003). A method for structural dynamic contact problems with friction and wear. *International Journal for Numerical Methods in Engineering* **58**, 2371-2385.

Strömberg, N. (2005). An implicit method for frictional contact, impact and rolling. *European Journal of Mechanics A/Solids* **24**, 1016-1029.

Talon, C., Curnier, A. (2003). A model of adhesion coupled to contact and friction. *European Journal of Mechanics A/Solids* **22**, 545-565.

Wriggers, P., Mische, C. (1994). Contact constraints within coupled thermomechanical analysis - a finite element model. *Computer Methods in Applied Mechanics and Engineering* **113**, 301-319.